Observation and Phenomenological Interpretation of Shifts in Electrical Resonance of Square Shaped Planar THz Split Ring Resonators

Rahul Kumar[1], **Ankit Arora**[1], **Shaumik Ray**[2], **Bala Pesala**[2], **Enakshi Bhattacharya**[1], **and Ananth Krishnan**[1]

[1]Department of Electrical Engineering
Indian Institute of Technology Madras, Chennai 600036, India
[2]CEERI, CSIR Campus, Chennai 600113, India

Abstract— The electrical resonance in Square shaped planar THz Split Ring Resonators (*SqSRR*) is observed at all polarizations of the incident wave. This resonance has been conventionally attributed to dipole oscillations in the arms parallel to the incident E-field (vertical arm), while neglecting the effect of arm perpendicular to the incident E-field (horizontal arm) that has been described in the past as the cut-wire approximation. In order to study the effect of horizontal arm on electrical resonance, several geometrical modifications of *SqSRR* consisting of identical vertical arms with varying horizontal arm lengths, were designed, fabricated and characterized at frequencies from 0.1 to 0.3 THz, at normal incidence. Contrary to the cut wire approximation, significant shift in electrical resonance frequency was observed with varying horizontal arm lengths of *SqSRR*. The presented experimental results and analysis based on the surface current profile in these structures, indicate the necessity to include the effect of horizontal arm in design of *SqSRR*. The shifts in plasma frequency with variation in horizontal arm length is explained as dilution of the effective electron density of the vertical arm. Simple modification in existing models for plasma frequency and electrical resonance frequency is proposed to consider the effect of horizontal arm lengths. Experimental and simulated results were found to be in good agreement with the proposed model.

1. INTRODUCTION

The first experimental demonstration of negative index material was achieved at microwave frequency by using periodic arrangement of circular Split Ring Resonator (*SRR*) structures (for negative effective relative permeability (μ_r)) and thin metallic wires (for negative effective relative permittivity (ϵ_r)) in alternating layers [1]. Since the first experimental demonstration, several efforts have been made to increase the operating frequency of SRR by reduction of size or by modification of shapes of *SRR* or both [2–5]. Among these structures, square shaped *SRR* (*SqSRR*) is one of the popular geometries because of the ease in micro and nanoscale fabrication of Cartesian structures [2–5]. However, apart from the magnetic resonance, *SqSRR* also exhibit an electrical resonance in all the orientations [3, 6]. This resonance is attributed to oscillatory current in the vertical arm and generally referred to as the cut-wire approximation of *SqSRR* [3, 6]. To the best of our knowledge, thus far, in the cut-wire approximation, the effect of horizontal arms has always been neglected. In this work, we have designed, fabricated and characterized several modifications of planar *SqSRR* to experimentally investigate the effect of horizontal arm length on electrical resonance for frequencies from 0.1 to 0.3 THz at normal incidence. We show that, though in electrical resonance the vertical arms play dominant role, effect of horizontal arm length can not be neglected. We have also provided a simple modification factor in the analytical expression of the plasma frequency ($f_p = \omega_p/2\pi$) given in [7] and electrical resonance frequency (f_0) given in [8] to explain the blue shift in electrical resonance with decrease in horizontal arm length. The modified analytical models were found to be in good agreement with experimental and simulated frequency of minimal transmission f_m. These results provide a better insight into the electrical resonance and will be helpful in designing *SqSRR* based filters in THz frequencies (0.1 to 10 THz) [9] for applications like sensing, security systems, imaging, explosive detection [10–12], etc..

2. METHODOLOGY

The geometrical parameters of *SqSRR* exhibiting resonances in THz region were determined by commercial full wave Maxwell's equation solver [13]. The top view of the unit cell along with optimized geometrical parameters of *SqSRR* suitable for the experimental setup is shown in Fig. 1(a).

The boundary conditions of unit cell used in simulation to maintain the incident polarization (shown by red arrows in Fig. 1(a)) are same as mentioned in [14]. The refractive index of glass substrate at frequencies ranging from 0.1 THz to 0.3 THz was taken as 2.45 [15]. $SqSRR$ was defined using 120 nm thick gold layer with a conductivity of 58×10^6 S/m [16].

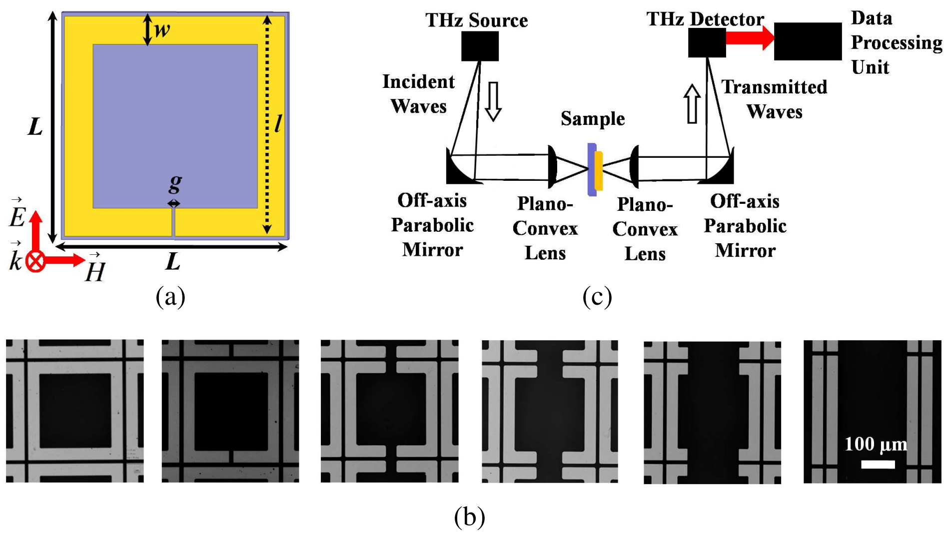

Figure 1: (a) Top view of unit cell along with incident wave polarization (shown in red arrows). Geometrical parameters are: unit cell length $L = 288$ µm, metal arm length $l = 280$ µm, arm width $w = 36$ µm, slit width $g = 8$ µm, metal thickness $t = 120$ nm, substrate thickness $t_{sub} = 180$ µm. (b) Micro graphs of some of the fabricated structures. Common scale is shown in the last micro graph. (c) Schematic of the characterization setup.

Structures corresponding to optimized geometrical dimensions were fabricated on ≈ 18 mm $\times$ 18 mm $\times$ 180 µm glass substrate. A 20 mm thick Cr layer for adhesion followed by a 120 mm thick Au layer was deposited using electron beam evaporation at 100°C. The deposited Cr/Au layers were patterned using UV photolithography technique followed by wet etching to obtain the final structures. The top views of some of the fabricated structures are shown in Fig. 1(b).

A Continuous-Wave THz transmitter/receiver arrangement (Toptica Photonics AG) was used to obtain transmission characteristics of fabricated structures. The schematic of the characterization setup is shown in Fig. 1(c). The obtained photocurrents were normalized w.r.t. the photocurrents of a bare glass wafer of same thickness.

3. RESULTS AND DISCUSSION

Experimental transmission characteristics of Closed Ring (CR) and $SqSRR$ from 0.1 THz to 0.3 THz shows a single dip in transmission occuring at ≈ 0.162 THz and ≈ 0.164 THz respectively, as shown in Fig. 2(a). In order to establish the exact mechanism of resonance, the instantaneous surface current density of CR and $SqSRR$ were calculated at f_m (shown in Fig. 2(b)). It can be seen that, the surface current density in vertical arms are oscillatory in nature, going from bottom to top as shown (or bottom to top depending on the phase of incident E-field, not shown in Figure). In literature, this current has been attributed to dipole oscillation of electrons of vertical arm, in presence of incident E-field. The corresponding resonance is termed as the electrical resonance, as this resonance is due to coupling of incident E-field with structures under study. In earlier reports, only vertical arms were considered to be participating in electrical resonance, therefore the electrical response of CR and $SqSRR$ were approximated to be equivalent to a cut-wire geometry as shown in Fig. 2(c). But, on meticulously analyzing the instantaneous surface current densities of CR and $SqSRR$ (shown in Fig. 2(b)), the electrons seem to be moving into horizontal arm from the bottom extrema of vertical arms and out of horizontal arm at top extrema of vertical arms. The possible reason for this current can be the movement of electrons in horizontal arms in response of the creation of a potential gradient along horizontal arms due to momentary charge accumulation in the vertical arms at the top and bottom (as shown in Fig. 2(d)). This movement of electrons reduces the net concentration of charges accumulated in vertical arms.

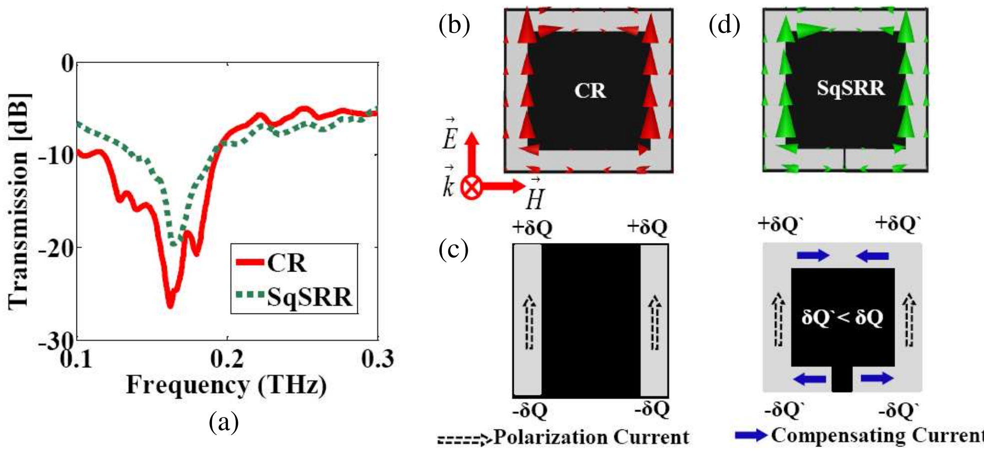

Figure 2: (a) Experimental transmission characteristics of CR and $SqSRR$. (b) Instantaneous surface current profile of CR and $SqSRR$ at frequency of minimum transmission f_m. Polarization of incident EM waves is given in red color arrows. (c) Conventional Cut-wire approximation. (d) Modified model after taking horizontal arm into consideration. Accumulated charges at tip of vertical arm will be diluted be due to presence of surface current in horizontal arm.

The simulated transmission characteristics of $SqSRR$ with decreasing horizontal arm length, shown in Fig. 3(a), shows the significant blue sift in resonance frequency, i.e., moving from closed ring to vertical stripes. To understand the physical phenomenon behind this blue shift, we started with the plasma frequency expression (ω_p) for periodic structures of thin wires given in [7] by Eq. (1).

$$\omega_p^2 = \frac{n_{\mathit{eff}}\, e^2}{\epsilon_0 m_{\mathit{eff}}} \tag{1}$$

where n_{eff} is effective electron density in a unit cell, e is charge of electron, m_{eff} is effective mass of electron and ϵ_0 is permittivity of free space. In case of $SqSRR$, if the effect of the horizontal arms are neglected, the effective electron density n_{eff} can be given as,

$$n_{\mathit{eff}} = 2 \times n \frac{lw}{L^2} \tag{2}$$

where n is electron density in bulk medium, l is length, w is width and L is lattice constant (refer to Fig. 1(a)). The factor of 2 comes in the equation due to the presence of 2 vertical arms that are symmetric about the vertical axis. In this study, all $SqSRR$ structures considered were symmetric about vertical axis and asymmetric modifications even though possible are not considered for simplicity. If the effect of horizontal arms are considered, n_{eff} will decrease due to flow of accumulated charges from vertical arms into the horizontal arms. In Eq. (1), m_{eff} is assumed to be constant for all the variation of horizontal arms, as in all cases, the surface current densities in vertical arms are of the same order. Due to the vertical symmetry, let us consider only the left half of the unit cell. Now, assuming uniform distribution of electrons over the entire length of metal in the left half of the unit cell (as electron will quickly redistribute along horizontal arm to nullify potential gradient), the effective metal length on left half of unit cell can be rewritten as
Effective Metal Length = Vertical Arm length + Top Horizontal Arm Extension + Bottom Horizontal Arm Extension

$$\text{Each horizontal arm extension} = \frac{l}{2} - w - \frac{g}{2}$$
$$\text{Effective Metal Length} = 2l - 2w - g$$

Now, the effective electron density will be reduced and let it be denoted by ($n_{\mathit{eff}_{modified}}$).

$$n_{\mathit{eff}_{modified}} = n_{\mathit{eff}} \times \frac{l}{(2l - 2w - g)} \tag{3}$$

where g is gap width. In case of vertical stripes (cut-wire), the above modification will reduce to Eq. (2). On substituting Eq. (3) in Eq. (1) and representing it in terms of cut-wire plasma frequency we get,

$$\omega^2_{p_{modified}} = \omega^2_{cutwire} \frac{l}{(2l - 2w - g)} \tag{4}$$

where,

$$\omega^2_{cutwire} = \frac{n_{eff} e^2}{\epsilon_0 m_{eff}}. \tag{5}$$

Also due to finite length of vertical arm, ϵ_r is negative between f_0 and f_p [8]. This lower cut-off frequency (f_0) has been empirically derived in [8] as,

$$f_0 = [c_{light}/\sqrt{2\pi} l] \times [a_0 ln(l/\Delta) + a_1]^{-1/2} \tag{6}$$

where c_{light} is speed of light in vacuum, Δ is separation between vertical arm of adjacent unit cells, a_0 and a_1 are fitting parameters. Since, we have assumed uniform distribution of electrons over the entire length of metal, l in the above expression can be modified as,

$$f_{0_{modified}} = [c_{light}/\sqrt{2\pi}(2l - 2w - g)] \times [a_0 ln((2l - 2w - g)/\Delta) + a_1]^{-1/2} \tag{7}$$

In order to experimentally validate the effect of horizontal arm length, several $SqSRR$ structures with varying horizontal arm length were fabricated and characterized. Variation of modified plasma frequency ($f_{p_{modified}} = \omega_{p_{modified}}/2\pi$), modified resonant frequency($f_{0_{modified}}$), f_m after normalizing w.r.t. their cut-wire response as function of horizontal length are plotted in Fig. 3(b). It can be seen that they are in good agreement. Mismatch between experimental and simulated results is attributed to the difference in material constants and fabrication tolerances.

Same concept can be extended to explain the origin of negative epsilon in case of EEMR [17]. Due to asymmetry along the direction of external E-field, at EEMR the charge gradient in one arm dominates over other, thus giving raise to circulating current.This circulating current leads to the distribution of effective electrons over the complete circumference of $SqSRR$, resulting in substantial reduction of plasma frequency.

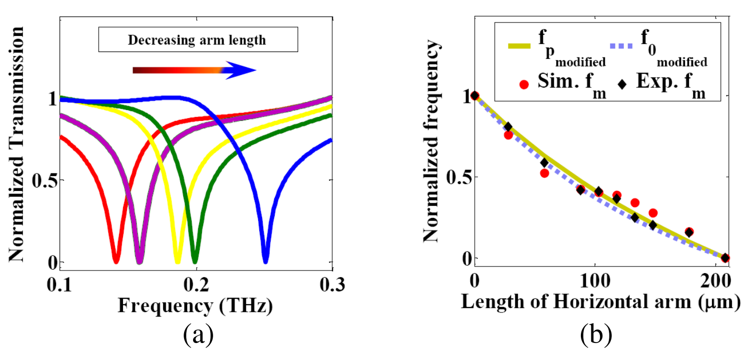

Figure 3: (a) Simulation showing blue shift in normalized transmission spectra with decrease in length of horizontal arm. Red color and Blue color transmission spectra corresponds to CR and vertical strips respectively. (b) Normalized modified plasma frequency ($f_{p_{modified}}$), electrical resonance frequency ($f_{0_{modified}}$) and the corresponding transmission (f_m) versus length of horizontal arm. These frequencies are normalized w.r.t. the corresponding cut-wire response.

4. CONCLUSION

We have investigated the effect of horizontal arm length on electrical resonance. We showed that, contrary to conventional cut-wire approximation, the horizontal arm plays a significant role in determining the electrical resonance by providing path for flowing of momentarily accumulated charges at ends of the vertical arm into horizontal arm. We modelled this effect, assuming uniform distribution of electrons over the entire length of metal and found it to be in good agreement with simulated and experimental results. These results will be helpful in better designing of $SqSRR$ for various applications like filters, sensors, etc. in THz frequencies.

ACKNOWLEDGMENT

Author would like to acknowledge NPMASS for providing HFSS license and CNNP for providing fabrication facilities.

REFERENCES

1. Smith, D. R., W. J. Padilla, D. C. Vier, S. C. Nemat-Nasser, and S. Schultz, "Composite medium with simultaneously negative permeability and permittivity," *Physical Review Letters*, Vol. 84, No. 18, 4184, 2000.
2. Dolling, G., M. Wegener, C. M. Soukoulis, and S. Linden, "Negative-index metamaterial at 780 nm wavelength," *Optics Letters*, Vol. 32, No. 1, 53–55, 2007.
3. Linden, S., C. Enkrich, M. Wegener, J. Zhou, T. Koschny, and C. M. Soukoulis, "Magnetic response of metamaterials at 100 terahertz," *Science*, Vol. 306, No. 5700, 1351–1353, 2004.
4. Kafesaki, M., I. Tsiapa, N. Katsarakis, T. Koschny, C. M. Soukoulis, and E. N. Economou, "Left-handed metamaterials: The fishnet structure and its variations," *Physical Review B*, Vol. 75, No. 23, 235114, 2007.
5. Shalaev, V. M., "Optical negative-index metamaterials," *Nature Photonics*, Vol. 1, No. 1, 41–48, 2007.
6. Koschny, T., M. Kafesaki, E. N. Economou, and C. M. Soukoulis, "Effective medium theory of left-handed materials," *Physical Review Letters*, Vol. 93, No. 10, 107402, 2004.
7. Pendry, J. B., A. J. Holden, W. J. Stewart, and I. Youngs, "Extremely low frequency plasmons in metallic mesostructures," *Physical Review Letters*, Vol. 76, No. 25, 4773, 1996.
8. Koschny, Th, P. Marko, D. R. Smith, and C. M. Soukoulis, "Resonant and antiresonant frequency dependence of the effective parameters of metamaterials," *Physical Review E*, Vol. 68, No. 6, 065602, 2003.
9. Ferguson, B. and X.-C. Zhang, "Materials for terahertz science and technology," *Nature Materials*, Vol. 1, No. 1, 26–33, 2002.
10. Yen, T.-J., W. J. Padilla, N. Fang, D. C. Vier, D. R. Smith, J. B. Pendry, D. N. Basov, and X. Zhang, "Terahertz magnetic response from artificial materials," *Science*, Vol. 303, No. 5663, 1494–1496, 2004.
11. Fitzgerald, A. J., E. Berry, N. N. Zinovev, G. C. Walker, M. A. Smith, and J. M. Chamberlain, "An introduction to medical imaging with coherent terahertz frequency radiation," *Physics in Medicine and Biology*, Vol. 47, No. 7, R67, 2002.
12. Federici, J. F., B. Schulkin, F. Huang, D. Gary, R. Barat, F. Oliveira, and D. Zimdars, "THz imaging and sensing for security application sexplosives, weapons and drugs," *Semiconductor Science and Technology*, Vol. 20, No. 7, S266, 2005.
13. High Frequency Structural Simulator (HFSS).
14. Yasar-Orten, P., E. Ekmekci, and G. Turhan-Sayan, "Equivalent circuit models for split-ring resonator arrays," *PIERS Proceedings*, 534–537, Cambridge USA, July 5–8, 2010.
15. Naftaly, M. and R. E. Miles, "Terahertz time-domain spectroscopy for material characterization," *Proceedings-IEEE*, Vol. 95, No. 8, 1658, 2007.
16. HFSS material data base.
17. Katsarakis, N., T. Koschny, M. Kafesaki, E. N. Economou, and C. M. Soukoulis, "Electric coupling to the magnetic resonance of split ring resonators," *Applied Physics Letters*, Vol. 84, No. 15, 2943–2945, 2004.